Macromolecular Bioscience
www.mbs-journal.de

Fabrication of Stiffness Gradients of GelMA Hydrogels Using a 3D Printed Micromixer

Antonina Lavrentieva, Tabea Fleischhammer, Anton Enders, Hamidreza Pirmahboub, Janina Bahnemann, and Iliyana Pepelanova*

Many properties in both healthy and pathological tissues are highly influenced by the mechanical properties of the extracellular matrix. Stiffness gradient hydrogels are frequently used for exploring these complex relationships in mechanobiology. In this study, the fabrication of a simple, cost-efficient, and versatile system is reported for creation of stiffness gradients from photoactive hydrogels like gelatin-methacryloyl (GelMA). The setup includes syringe pumps for gradient generation and a 3D printed microfluidic device for homogenous mixing of GelMA precursors with different crosslinker concentration. The stiffness gradient is investigated by using rheology. A co-culture consisting of human adipose tissue-derived mesenchymal stem cells (hAD-MSCs) and human umbilical cord vein endothelial cells (HUVECs) is encapsulated in the gradient construct. It is possible to locate the stiffness ranges at which the studied cells displayed specific spreading morphology and migration rates. With the help of the described system, variable mechanical gradient constructs can be created and optimal 3D cell culture conditions can be experientially identified.

1. Introduction

Cellular fate is strongly influenced by mechanical cell–matrix interactions and by the composition of the tissue microenvironment. Most cell types, including mesenchymal stem cells (MSCs), are able to sense physical characteristics of their external microenvironment and convert them to intracellular biochemical signals. MSCs have been shown to express mechanoreceptors and to actively respond to mechanical stimulation, which can influence cell fate.[1] Indeed, numerous studies have revealed the influence of hydrogel mechanical properties on cell behavior.[2–4] Hydrogels with different stiffness and porosity remain a popular 3D cultivation platform for tissue engineering, in vitro modeling and drug screening.[5]

Although bulk hydrogels with a variable stiffness do provide a platform for different cell types and applications, they are limited as a screening platform for the identification of optimal cell niche and cultivation conditions.[6,7] As a result, in vitro reproduction of mechanical and hydrogel-composition gradients could be a useful tool for tissue models and tissue engineering.[8–11] Indeed, starting from early embryogenesis, gradients play a key role in various processes, including determination of cell fate over the entire lifespan of an organism. For example, in vivo gradients can be physiological or pathological, stable, or transient. Physical gradients (topology, stiffness, and porosity) represent a driving force for complex biological activities, including cell differentiation and migration.[12] Typical examples of tissues with physical gradients are cartilage, bones, and teeth.[11,13,14] Pathological mechanical gradients can be found in tumors,[15] scars,[16,17] and wounds.[17] Therefore, it is essential to recreate an in vivo-like mechanical cell microenvironment for the successful study of physiological and pathological processes in vitro. To that end, the fabrication of gradient hydrogels can fulfill two important roles: 1) the in vitro recreation of in vivo gradients for modeling and tissue engineering and 2) the establishment of a screening system for optimization of 3D cell culture conditions.

The scientific literature lists many methods which can be used to create a hydrogel with a mechanical gradient.[18,19] The choice for the specific fabrication technique is usually related to the type of hydrogel used in the study, as well as the available equipment in laboratories. Stiffness gradients from photo-crosslinkable hydrogels (such as gelatin-methacryloyl (GelMA) or polyacrylamide) are usually created by varying the photopolymerization step via photomasking or photolithography.[20] Disadvantages of these techniques stem from reproducibility issues[21] and the necessity for specialized photolithography facilities. Another approach to create gradient stiffness in photo-crosslinkable hydrogels is to create a concentration gradient first, by the use of passive diffusion[22] or the dynamic mixing of two precursor materials with varying crosslinker

Dr. A. Lavrentieva, T. Fleischhammer, A. Enders, Dr. J. Bahnemann, Dr. I. Pepelanova
Institute of Technical Chemistry
Leibniz University of Hannover
Callinstrasse 5, Hannover 30167, Germany
E-mail: lavrentieva@iftc.uni-hannover.de
H. Pirmahboub
Institute of Cell Biology and Biophysics
Leibniz University of Hannover
Herrenhäuser Str. 2, Hannover 30419, Germany
The ORCID identification number(s) for the author(s) of this article can be found under https://doi.org/10.1002/mabi.202000107.

DOI: 10.1002/mabi.202000107

concentration,[23] followed by a single uniform exposure to light for crosslinking. We selected the second approach, because of its superior reproducibility and because this strategy ensures all cells have been exposed to identical crosslinking conditions and differ in their response to the stiffness gradient only. Moreover, the dynamic mixing method is more versatile, allowing the system to be used not only for mechanical gradients from photo-crosslinkable precursors, but also provides the flexible opportunity for the introduction of a secondary gradient in a straightforward manner, by simply adding a biochemical signal[24] (e.g., growth factors, adhesion molecules) or a different cell type in one precursor solution.

In this study, we report the fabrication of a GelMA gradient hydrogel. The gradient was created by using syringe pumps mixing two different GelMAs, synthesized from the same gelatin batch, but differing in crosslinker amount (i.e., in their degree of functionalization, DoF).[23] We designed a microfluidic device for efficient and homogenous mixing of the GelMA precursors. The micromixer was produced by 3D printing and does not require polydimethylsiloxane (PDMS) interfaces or access to clean room facilities.[25] The stiffness gradient resulting throughout the macroscale 3D construct was studied by determining the mechanical hydrogel properties of collected fractions using rheology. We then encapsulated a cell model of human adipose tissue-derived mesenchymal stem cells (hAD-MSCs) and human umbilical cord vein endothelial cells (HUVECs) in the stiffness gradient system. We were especially interested in screening the mechanical conditions under which these cell types start displaying changes in morphology and cell spreading. We have created a simple, open-source system for the creation of stiffness gradients which is applicable to other photoactive hydrogel materials, and which can be adapted in a versatile manner to include an additional gradient for multidimensional exploring of the sweet spot of a particular cellular niche.

2. Experimental Section

2.1. Mixer and Casting Mold Design and Printing

To mix the hydrogels, a passive micromixer was designed using the Solidworks CAD software (Dassault systems, France). The HC Mixer design[26] was chosen for its high efficiency,[25] and it only required the constant flow of fluids to facilitate proficient mixing. At the end of the mixer section, a broad opening was designed to create an evenly spread hydrogel outflow. In addition, a simple reservoir was designed as a casting mold to collect the hydrogel from the mixer. Mixer and casting mold dimensions and CAD-files are available in the Supporting Information (**Figure 1**; Figure S1, Supporting Information).

Both the micromixer and the casting mold were fabricated via MultiJet 3D printing (MJP 2500 Plus, 3D Systems Inc., USA) from M2-RCL printing material and M2-SUP support material (3D Systems Inc., USA). After printing, the resulting objects were placed in water steam to melt the support material. Residues of the support material were dissolved in paraffin oil (Carl Roth GmbH und Co. KG, Germany) at 65 °C. Mixer channels were flushed with oil as well. Afterward, the oil was removed by flushing the mixer channels with soap water (heated at 65 °C). Disinfection of the 3D-printed parts was performed using ethanol (70%, v/v, 1 h) according to Siller et al.[27]

2.2. GelMA Hydrogels

GelMA was synthesized from the same gelatin material batch as previously described,[6] using the protocol of Shirahama et al.[28] The low DoF GelMA material had a DoF of 27%, while the high DoF material displayed a derivatization of 98%, as determined by the 2,4,6-trinitrobenzene sulfonic acid assay.[28] The

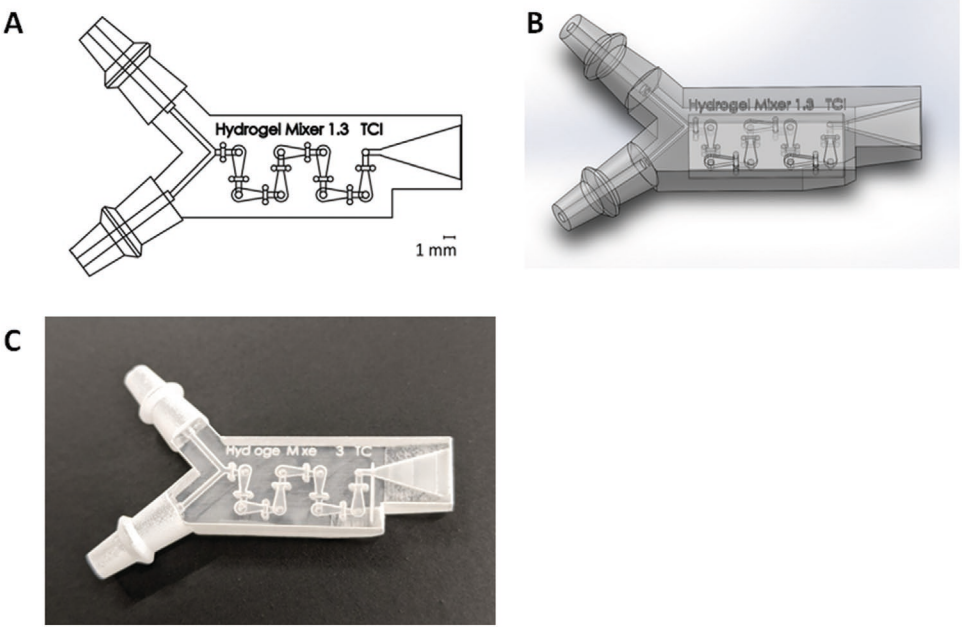

Figure 1. A) Schematic drawing of the micromixer, B) CAD 3D model of the micromixer, C) 3D-printed micromixer.

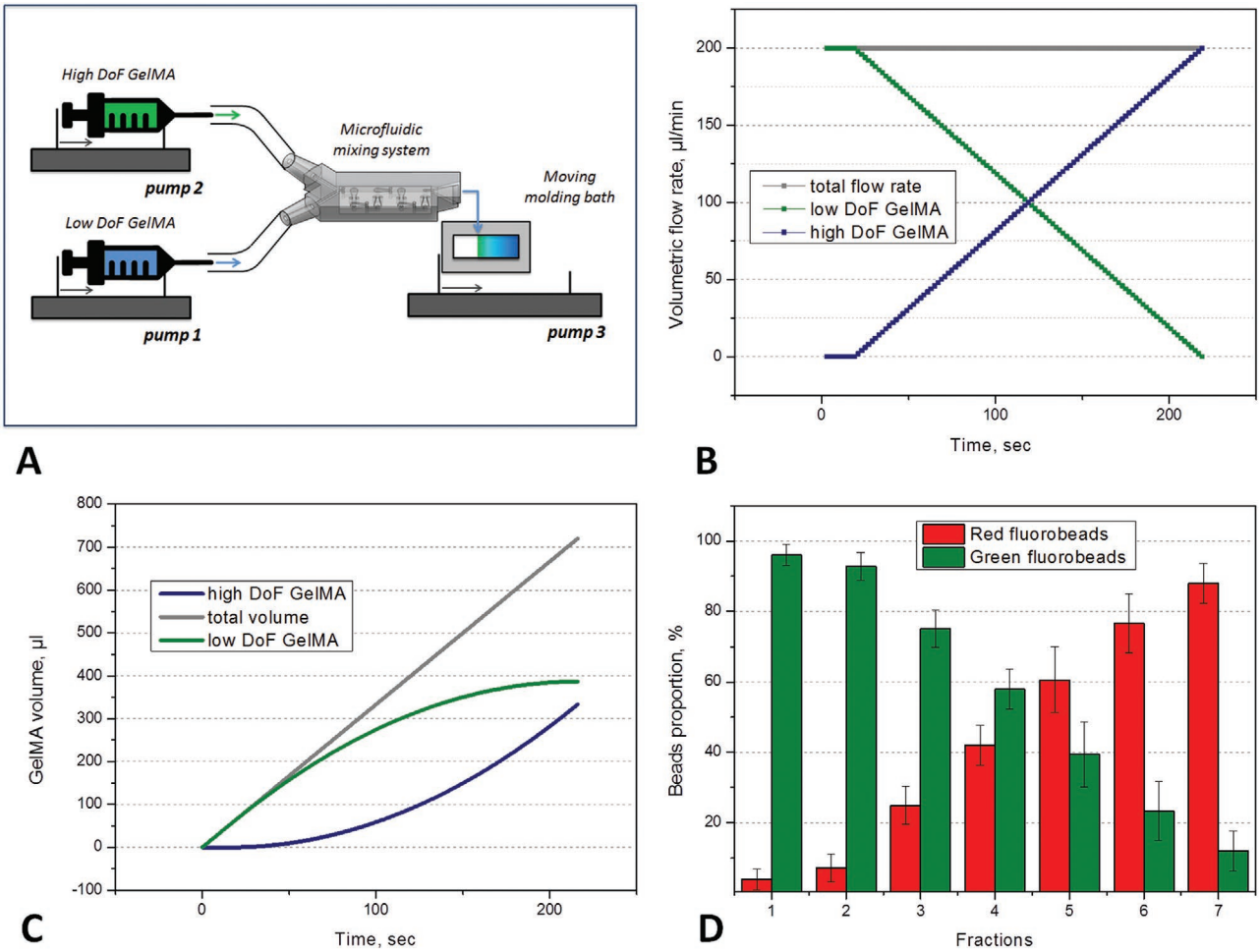

Figure 2. Schematic representation of the gradient fabrication system and dynamic mix analysis. A) Schematic representation of the gradient making three-pump system. B) Programmed flow profiles (volumetric flow rates) of the pumping system. C) Time profiles of the low DoF, high DoF, and total GelMA pumped volumes. D) Proportions of green and red beads in the gradient fractions measured by flow cytometry.

hydrogels were both prepared at a concentration of 5% (w/v) by weighing the appropriate amount of GelMA and dissolving in phosphate-buffered saline (PBS) at 37 °C until complete dissolution. Irgacure2959 (2-hydroxy-4′-(2-hydroxyethoxy)-2-methylpropiophenone) was added as a photoinitiator to a final concentration of 0.1% (w/v).

2.3. Pump Programming and Fraction Collection

A syringe pump system was used for the creation of the GelMA gradients. Syringe pumps (Alladin AL 1000, World Precision Instruments Inc., USA) were programmed in a manner similar to the experimental setup of Jeon et al.[24] and Singh et al.,[29] where two different flow profiles were applied: pump 1 (with a starting flow rate of 200 µL min^{-1} and decreasing in a linear manner down to 0 µL min^{-1}) and pump 2 (with a starting flow rate of 0 µL min^{-1} and increasing in a linear fashion up to 200 µL min^{-1}), with both pumps featuring a constant sum flow rate of 200 µL min^{-1} (**Figure 2**A,B). A third pump was used to move the casting mold with a continuous speed of 120 µL min^{-1} (Figure 2A). This setting results in a velocity of 10 mm min^{-1} when using a 1 mL syringe. In order to prevent thermoreversible GelMA gelation as a result of decreasing temperature during operation, the mixer and both pumps with hydrogel-containing syringes were placed under a ceramic 250 W infrared lamp (Elstein, Northeim, Germany). Time profiles of the low DoF, high DoF, and total GelMA pumped volumes were calculated as cumulative volumes over the entire program time (Figure 2C). Gradient hydrogel fractions were collected in 1.5 mL microtubes during the entire pump program every 45 s.

2.4. Gradient Characterization with Flow Cytometric Analysis of Fluorescent Beads Suspension

To characterize the mixer, as well as the resulting gradient composition, green fluorescent beads (BD CelibriteTM 3-color kit, Becton Dickinson, Franklin Lakes, NJ, USA) were resuspended in low DoF GelMA and red fluorescent beads (BD CelibriteTM 3-color kit, Becton Dickinson, Franklin Lakes, NJ, USA) were resuspended in high DoF GelMA. The pump program was started and collected fractions were analyzed by BD Accuri C6 (Becton Dickinson, Franklin Lakes, NJ, USA) using a 488 nm

Argon-ion laser. The green fluorescence light of particles was collected by a 530 nm filter and the red fluorescence by a 675 nm filter, respectively. At least 10 000 events per sample were analyzed with the BD Accuri C6 Software (v. 1.0, Becton Dickinson, Franklin Lakes, NJ, USA).

2.5. Rheology

Hydrogel fractions were numerated in the order of their collection. The mechanical stiffness of the GelMA hydrogels was determined at 37 °C by using oscillatory rheology with a MCR 302 modular rheometer (Anton Paar, Austria) equipped with plate–plate geometry (20 mm diameter plate). Polymerization was performed by in situ crosslinking via UV irradiation from below (Delolux 80, Delo, Germany), with a light intensity of 20 mW cm^{-2} and UV irradiation time of 5 min. Storage and loss moduli were recorded in a time sweep oscillatory test under a constant strain amplitude of 1% and at a constant frequency of 1 Hz, which is within the linear viscoelastic (LVE) region of the GelMA hydrogel.

2.6. Cell Encapsulation in Hydrogel and Microscopy

hAD-MSCs were isolated from the adipose tissue of four donors following abdominoplasty (approved by the Institutional Review Board of the Hannover Medical School). The isolated cell populations have been previously extensively characterized as mesenchymal stem cells by surface marker analysis and functional properties. hAD-MSCs were cultivated in alpha-MEM medium (Thermo Fisher Scientific, Waltham, MA, USA) containing 1 g L^{-1} glucose, 2×10^{-3} M L-glutamine, 10% human serum (CC-pro, Oberdorla, Germany) and 50 µg mL^{-1} gentamicin (Merck KGaA, Darmstadt, Germany) and were thereafter harvested by accutase treatment (Merck KGaA, Darmstadt, Germany). HUVECs were purchased by Thermo Fischer (C01510C, Thermo Fischer Scientific, Waltham, MA, USA), cultivated in endothelial cell basal medium 2 (Promo Cell, Germany) and harvested by accutase treatment. All used cells were up to passage 5. For encapsulation 1 million cells per mL of each cell type were encapsulated in the collected hydrogel fractions with the help of a cross linker (BLX-365 BIO-LINK, 365 nm, Vilber Lourmat Deutschland GmbH). The UV intensity used for polymerization was 1.2 J cm^{-2}. Hydrogel constructs with co-cultures were cultivated in alpha-MEM medium (Thermo Fisher Scientific, Waltham, MA, USA) containing 1 g L^{-1} glucose, 2×10^{-3} M L-glutamine, 10% human serum (CC-pro, Oberdorla, Germany) and 50 µg mL^{-1} gentamicin (Merck KGaA, Darmstadt, Germany). Microscopic analysis was performed with the help of cell imaging multi-mode reader (Cytation 5, BioTek, USA) and Gen5 Image Prime software.

2.7. Fluorescent Staining in Hydrogel Constructs and Confocal Microscopy

After 1 week of co-culture in the corresponding gradient fractions, hydrogel constructs were washed twice in warm PBS for 1 h and then fixed for 1 h in 4% paraformaldehyde in PBS at room temperature. Following fixation, constructs were washed once more with PBS and soaked in 0.1% Triton X-100 in PBS for 30 min to permeabilize the cells' membrane. For actin cytoskeleton staining, hydrogels were blocked in 1% bovine serum albumin (BSA) for 1 h and 1:500 diluted Atto 488-phalloidin (Merck KGaA, Darmstadt, Germany) in 0.1% BSA in PBS solution was added for 1 h at room temperature. After actin staining, hydrogel constructs were incubated for 1 h in blocking buffer (0.2% Tween 20, 10% fetal calf serum, and 1% BSA in PBS). 30 µL of primary anti-PECAM-1 (CD31) antibody (polyclonal rabbit IgG, Santa Cruz, SC 1506R) diluted 1:100 in blocking buffer were added on top of each construct in wet chambers and left overnight at 4 °C. Afterward, constructs were washed twice for 1 h in PBS and 30 µL of secondary antibody (goat-anti rabbit Alexa Fluor 555, Thermo Fisher Scientific, Waltham, MA, USA) diluted 1:250 in PBS were applied on top of hydrogel constructs in wet chambers and left overnight at 4 °C. Finally, constructs were washed twice for 30 min in PBS and cell nuclei were stained for 15 min with DAPI (Merck KGaA, Darmstadt, Germany) diluted 1:1000 in binding buffer. Images were obtained with a Zeiss LSM 980 equipped with an Airyscan 2, updated with a new multiplex mode. This mode provides smart detection schemes, parallel pixel acquisition, and can acquire eight superresolution image lines with a high signal-to-noise ratio in a single sweep.[30]

2.8. Cell Migration in Gradient Fractions

One of the basic mechanisms of cell translocation during morphogenesis, wound repair, and cancer invasion is collective migration—a process in which cells move while retaining cell–cell contacts.[31] To evaluate cell migration in gradient GelMA fractions, cell aggregates of HUVEC and hAD-MSCs were encapsulated in hydrogel constructs as described above for co-cultures. In migration experiments, cell spheroids were made from either HUVECs or hAD-MSCs with the help of spherical plates 5D (Kugelmeier AG, Switzerland) (Video S1, Supporting Information). For spheroid formation, 0.5 million HUVECs or hAD-MSCs in 1 mL cell culture medium were seeded into the well and placed in the incubator overnight (see Videos in the Supporting Information). Each cell spheroid contained ≈670 cells and was ≈100 µm in diameter. After formation, spheroids were collected by centrifugation (3 min × 200 × g) and encapsulated in hydrogel fractions. Collective cell migration from the spheroid into the hydrogel was evaluated and measured after 48 h using a microscope (Olympus, IX50, Olympus Corporation, Tokyo, Japan) with a camera (Olympus SC30, IX-TVAD, Tokyo, Japan) and the cellSens Software (cellSens Standard 1.7.1, Olympus). Singular and isolated cells, detected on the surface of the gradient hydrogel constructs, were not considered for analysis, and only collectively migrating cells (i.e., cells retaining cell–cell contact) were evaluated.

2.9. Cell Viability after Passage through the Micromixer Channels

For evaluation of the influence of micromixer on cell viability, HUVECs or hAD-MSCs suspensions were prepared in cell

culture medium (10^5 cells mL^{-1}) or in low DoF GelMA hydrogel (10^6 cells mL^{-1}). Syringes of pump 1 and pump 2 were filled with cell suspension, and a full program run was performed, with cells collected into 2 mL Eppendorf tubes directly from the micromixer. Four replicates of cell suspension in cell culture medium (100 µL) were transferred to 96 well plates. A portion of the cell suspension was not pumped though the micromixer and served as a control. Cell viability in 2D was evaluated after 24 and 72 h with the help of CellTiter-Blue Assay (CTB, Promega, USA) according to the manufacturer's protocol. Briefly, 100 µL of 10% CTB solution (1:10 v/v stock solution in basal medium) was added to each well. After 1.5 h of incubation, fluorescence was measured at an extinction wavelength of 544 nm and an emission wavelength of 590 nm using a microplate reader (Fluoroskan Ascent, Thermo Fisher Scientific Inc., Waltham, MA, USA). Cell viability was also visualized by live/dead staining. Cells were incubated in 3 µm Calcein-AM (Merck, Darmstadt, Germany) and 2.5 µm propidium iodide (Merck, Darmstadt, Germany) solution in basal medium for 15 min at 37 °C and analyzed with a fluorescent microscope (Olympus, IX50, Olympus Corporation, Tokyo, Japan), equipped with a camera (Olympus SC30, IX-TVAD, Olympus Corporation, Tokyo, Japan) and the CellSens Software (CellSens Standard 1.7.1, Olympus Corporation, Tokyo, Japan).

Cell suspensions in hydrogels were polymerized in 50 µL constructs as described above (Section 2.6). Cell viability was also evaluated with the CTB assay and Calcein-AM/propidium iodide staining. For 3D cell cultures, hydrogel constructs were incubated in 400 µL CTB working solutions for 5 h.

2.10. Fabrication of a Co-Culture-Stiffness Gradient Construct

For the creation of the dual cell type-stiffness gradient construct, the designed casting mold form and the third pump were used (Figure 2A). The function of the third pump is a reproducible and constant movement of the casting mold with the speed of 50 mm min^{-1}. Blue labeled HUVECs (CellTracker Blue CMAC, Thermofischer) were resuspended in low DoF hydrogel and green labeled hAD-MSCs (Vybrant DiO Cell-Labeling Solution, Thermofischer) were resuspended in high DoF. After casting, the gradient construct was then polymerized with the help of a cross linker (BLX-365 Bio-Link, 365 nm, Vilber Lourmat, Germany) with a UV intensity of 1.2 J cm^{-2} and a polymerization time of ≈5 min and scanned using Cytation 5-cell imaging multi-mode reader (Biotek Instruments, Winooski, VT, USA).

3. Results and Discussion

3.1. Mixer Design and Printing

In order to mix the two GelMA hydrogels of distinct DoF in a reproducible and defined fashion, a passive microfluidic mixing system was developed. The HC mixer design was adapted from Viktorov et al.[26] for its high efficiency and ease of operation[25] and implemented in a 3D printed design with integrated silicon tube fitting for syringe connection and a widening opening for hydrogel outflow (Figure 1). This allows the mixed hydrogels to be cast evenly into a suitable 3D-printed casting mold reservoir. The microfluidic mixer provided efficient mixing of the two hydrogels in a closed system; (with a short residence time in the mixer itself) while relying solely on hydrogel movement inside the structured channel to achieve perfect mixing. The micromixer used in this study enables a homogeneous mixing of fluids in less than 1 s.[25] The small mixer size reduces the amount of hydrogel required to fill the mixer volume itself. Additionally, the smaller size makes the handling of syringe pumps and mixer module easier with restricted movement, e.g. a situation existing when working in a sterile environment (biosafety cabinet). At the same time, while the micromixer itself is small, it can be used to successfully generate macroconstructs at the centimeter scale.

It is important to emphasize that the micromixer is not used for gradient generation, like the microfluidic tree mixers used in many works. It solely ensures mixing of the gradient generated by the syringe pumps. Microfluidic tree mixers are frequently used for gradient generation.[32] These create a gradient perpendicular to the direction of flow. This means it is difficult to easily change the size of the resulting gradient or the scale of the overall construct, without creating a new device. In addition, one requires specialized PDMS equipment and clean room facilities for the manufacture of such devices. In contrast, the gradient created by dynamic mixing like the one described in this work is obtained in the direction of the flow. This allows a more flexible approach to gradient generation, because only a change in pump flow rates is required to create a larger or smaller hydrogel construct with a flatter/steeper gradient. The micromixer remains the same and no new manufacture is required.

3.2. Mixer and Pumping System Characterization: Flow Cytometry and Fluorescence Measurements

The two syringe pumps were programmed to start with linear flow rates (15 s, pump 1–200 µL min^{-1} and pump 2–0 µL min^{-1}) followed by linear increment of 2 µL min^{-1} for each pump (Figure 2B), which resulted in a linear increase of the total pumped volume and nonlinear calculated volumetric profiles for each hydrogel (Figure 2C). In order to evaluate the gradient-generating system, fluorescent microbeads were resuspended in the hydrogels. Green beads were added to low DoF GelMA and red beads were mixed with high DoF GelMA.

Since GelMA of different DoF possesses slightly different viscosities, this could have an influence on the speed of hydrogel syringe extrusion and hydrogel velocity within the mixer and, consequently, on the hydrogel composition after mixing. As can be seen in Figure 2D, particle composition in each fraction reflects the programmed pump profile (Figure 2B), with the proportion of green beads decreasing and red beads increasing in a linear manner.

To ensure the applicability of the micromixer for the manipulation of cell-laden hydrogels, cell viability was evaluated with both AD-MSCs and HUVECs after performing a full gradient program cycle. Cell viability was not affected by passage through the micromixer in both cell culture medium and in GelMA hydrogel and following 2D or 3D cultivation (see Figures S4 and S5 in the Supporting Information).

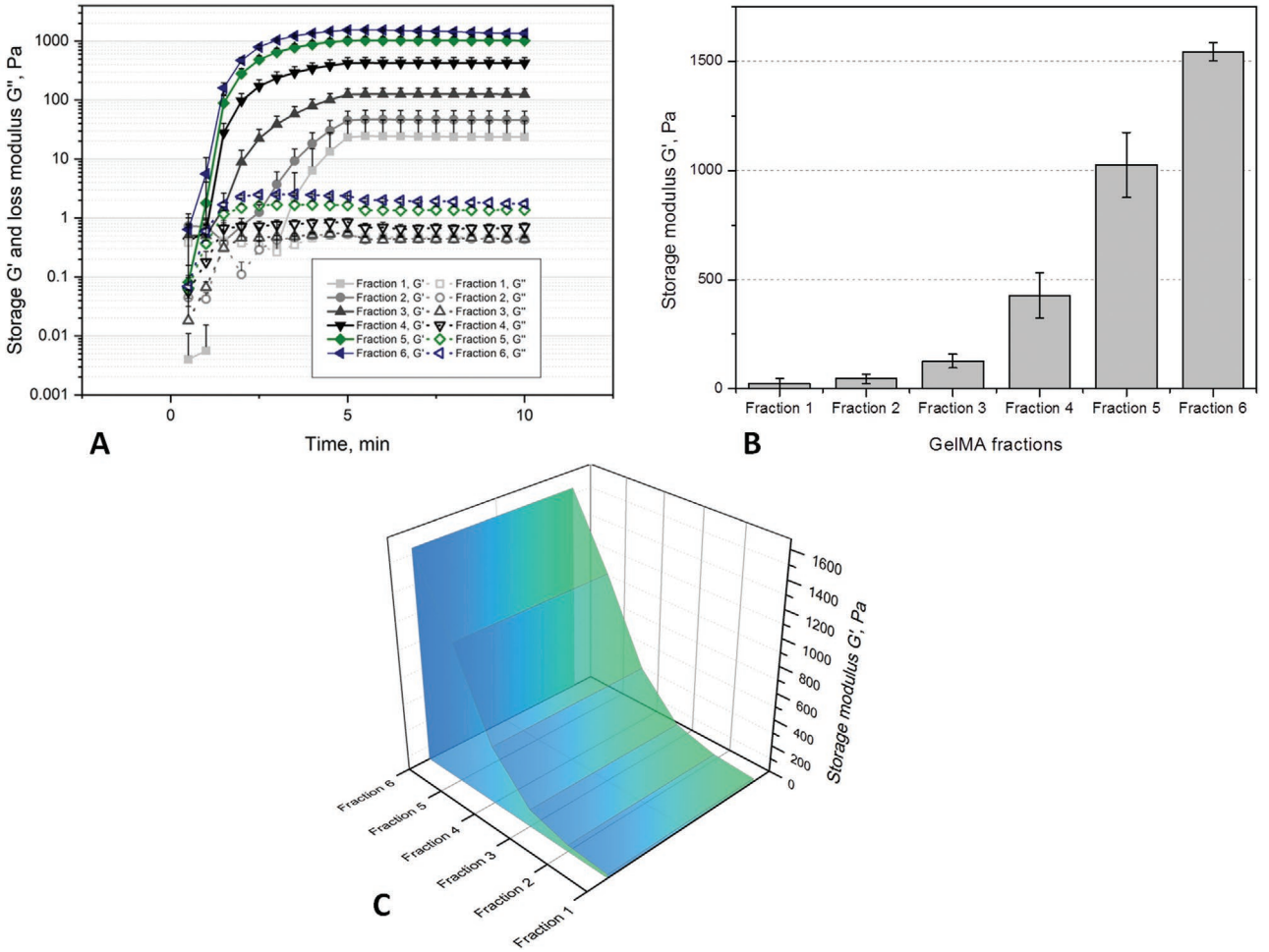

Figure 3. A) Crosslinking kinetics, B) final material stiffness (storage modulus, G′ and loss modulus, G″) of GelMA gradient fractions, and C) 3D representation of the changes in hydrogel stiffness along the fractions. Values shown are the result of triplicates from independent experiments.

3.3. Hydrogel Stiffness in GelMA Gradient Fractions

For gradient characterization, fractions were collected after starting the pump program. These fractions reflect the mechanical composition of the hydrogel at the corresponding spatiotemporal casting profile. The first collected fractions display lower mechanical strengths in comparison to fractions collected later. This is not surprising, since the gradient profile begins with a higher contribution of pump 1 which carries the low DoF material (see also Figure 2A). As the program proceeds, the contribution of pump 2 increases accordingly and the fraction of high DoF material in the construct rises. This is reflected by the higher storage moduli of later fractions. The increased contribution of the high DoF material to the overall mechanical profile of the hydrogel is also implicit in the crosslinking kinetics of the fractions, with earlier fractions exhibiting later polymerization, and later fractions displaying faster crosslinking, This behavior is explained by the increasing density of methacrylate and methacrylamide groups available for polymerization, since the fraction of material with high degree of functionalization increases as the casting program proceeds. Despite following a linear gradient of mixing, it is evident from **Figure 3**B that the resulting stiffness gradient profile is nonlinear. Even if the mass fraction of added hydrogel of high DoF is linear, the resulting contribution of additional methacrylate and methacrylamide groups still adds up to an exponential increase in mechanical strength (Figure 3C).

3.4. Cell Cultivation in GelMA Gradient Fractions

In order to expose the gradient to a cellular system, hAD-MSCs, and HUVECs were encapsulated as a co-culture in GelMA fractions and the resulting cell morphology was evaluated on days 1, 3, and 7 of cultivation. On day 7 of cultivation, hydrogel constructs were fixed, stained (with actin, CD31, and DAPI) and analyzed with the help of confocal microscopy. Representative Z-stacks of cells in gradient fractions after 3 days of cultivation can be seen in **Figure 4**A. Here, cell spreading can be seen in the first three fractions. These fractions demonstrate a mechanical stiffness ranging from 23.7 to 125.6 Pa. Cell spreading could already be observed on day 1 (24 h) of cultivation (Figure S2, Supporting Information), the extent of spreading decreased along the gradient.

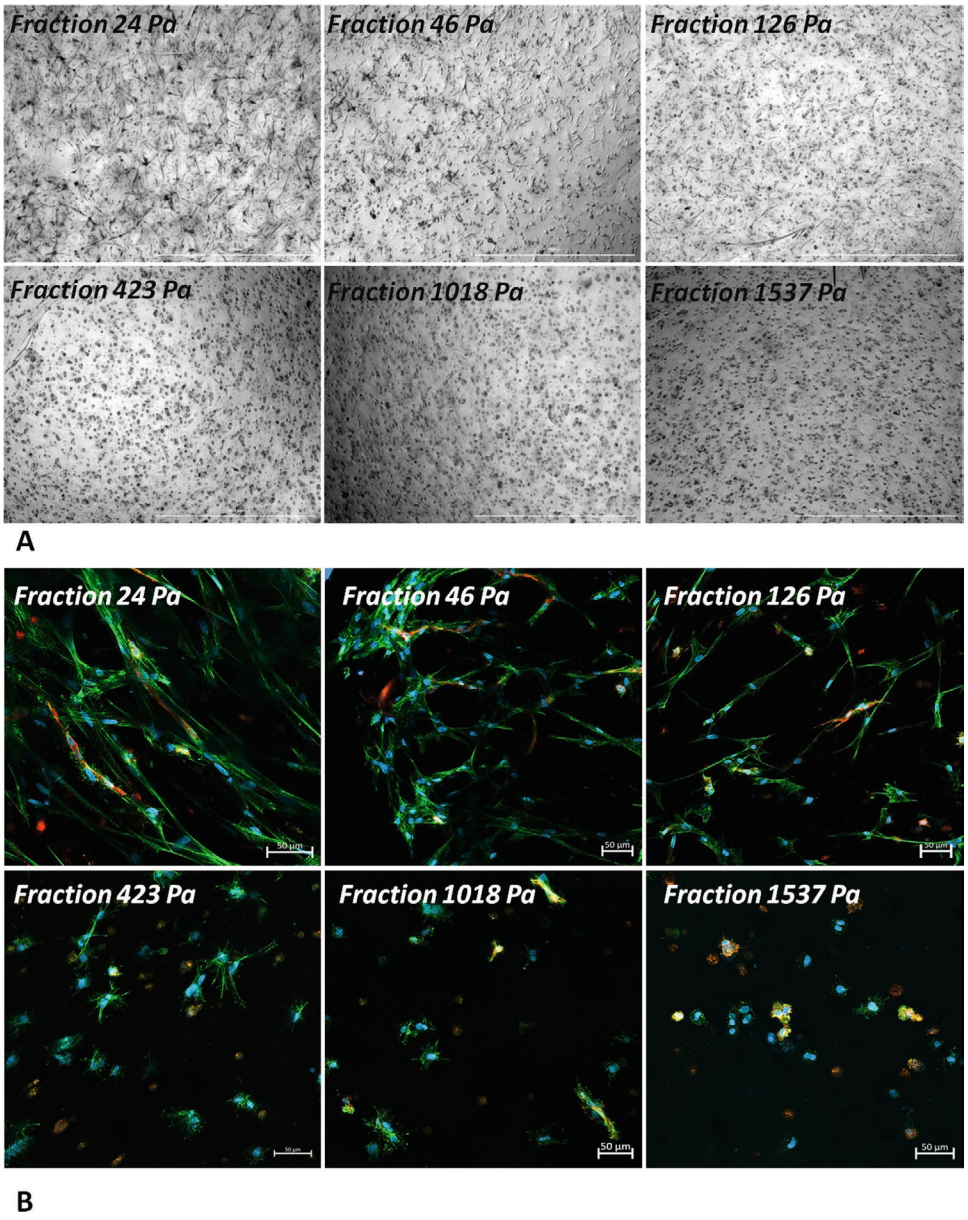

Figure 4. A) Microscopic analysis of hAD-MSCs and HUVECs co-culture after 3 days of cultivation in GelMA gradient fractions: Z-stack images were taken thought the entire hydrogel construct and reduced to one projection. Scale bar 1000 µm. B) Confocal microscopy of hAD-MSCs and HUVECs encapsulated in gradient fractions. Green staining, actin filaments; red staining, CD31; blue staining, DAPI, day 7 of cultivation.

Time-lapse microscopy of the cell growth in fraction one (23.7 Pa), fraction three (125.6 Pa), and fraction six (1536.7 Pa) support these observations, with good spreading already starting on day 1 of cultivation within fractions with 23.7 and 125.6 Pa, and no spreading observed in 1536.7 Pa (Videos S2–S4, Supporting Information). After 7 days of cultivation, actin staining confirmed decreased cellular spreading with increasing stiffness (Figure 4B). Additional staining with CD31 (red) was used to distinguish between hAD-MSCs and HUVECs, since only HUVECs express the CD31 antigen. Moreover, confocal microscopy revealed the difference in cell behavior of hAD-MSCs and HUVECs in the gradient fractions: HUVECs exhibit a mostly round morphology already in fraction with 125.6 Pa (red staining), while hAD-MSCs could still spread in this construct after 7 days of cultivation (Figure 4B). Some hAD-MSCs could spread even in the fraction with 423 Pa after 7 days of cultivation.

3.5. Cell Migration in Gradient Fractions

Similar to the observation of cell spreading in the gradient fractions, the distance of cell migration from imbedded spheroids continuously decreased with increasing stiffness (i.e., fraction number) (**Figure 5**; Figure S3, Supporting Information). Here as well, HUVECs were more sensitive to the increase of stiffness

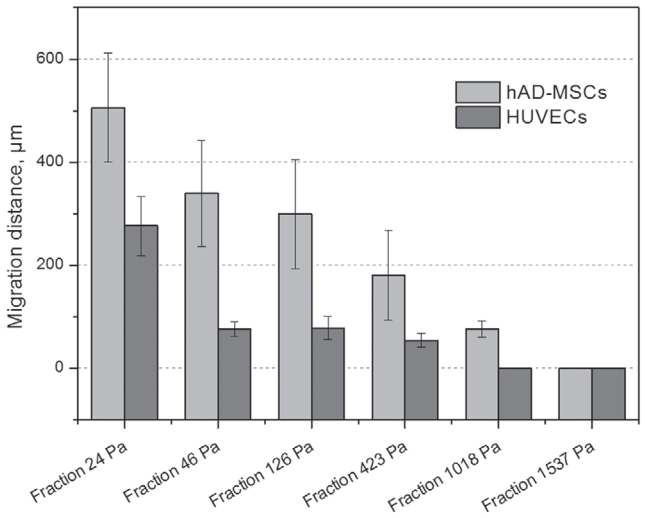

Figure 5. Evaluation of hAD-MSCs and HUVECs cell migration in GelMA gradient fractions after 48 h of cultivation. Distances of cell migration from spheroids imbedded in hydrogels were measured using CellSens Software (Olympus).

(i.e., decrease of the pore size)—and in comparison to the nearly linear decrease observed for MSCs migration, HUVECs migration distance was in general lower and dropped significantly already above a stiffness of 24 Pa. No outgrowth after 48 h of cultivation was observed for hAD-MSCs in 1536.7 Pa and for HUVECs in the range between 1017.7 and 1536.7 Pa.

3.6. Fabrication of a Dual Cell Type/Stiffness Gradient Construct

The macroscale 3D stiffness gradient construct with embedded co-culture cells was visualized using cell trackers (**Figure 6**). For this purpose, HUVECs stained with the blue cell tracker were resuspended in low DoF GelMA and hAD-MSCs stained with green tracker were resuspended in high DoF GelMA. The gradient hydrogel was dispensed from the micromixer into the moving molding cast and polymerized a described (Figure 2A). As can be seen in **Figure 7**, transitional gradient from blue-stained HUVECs (right end of the gel) to the green-stained hAD-MSCs (left end of the gel) was created with the three-pump system. A closer visual inspection of the cell distribution along

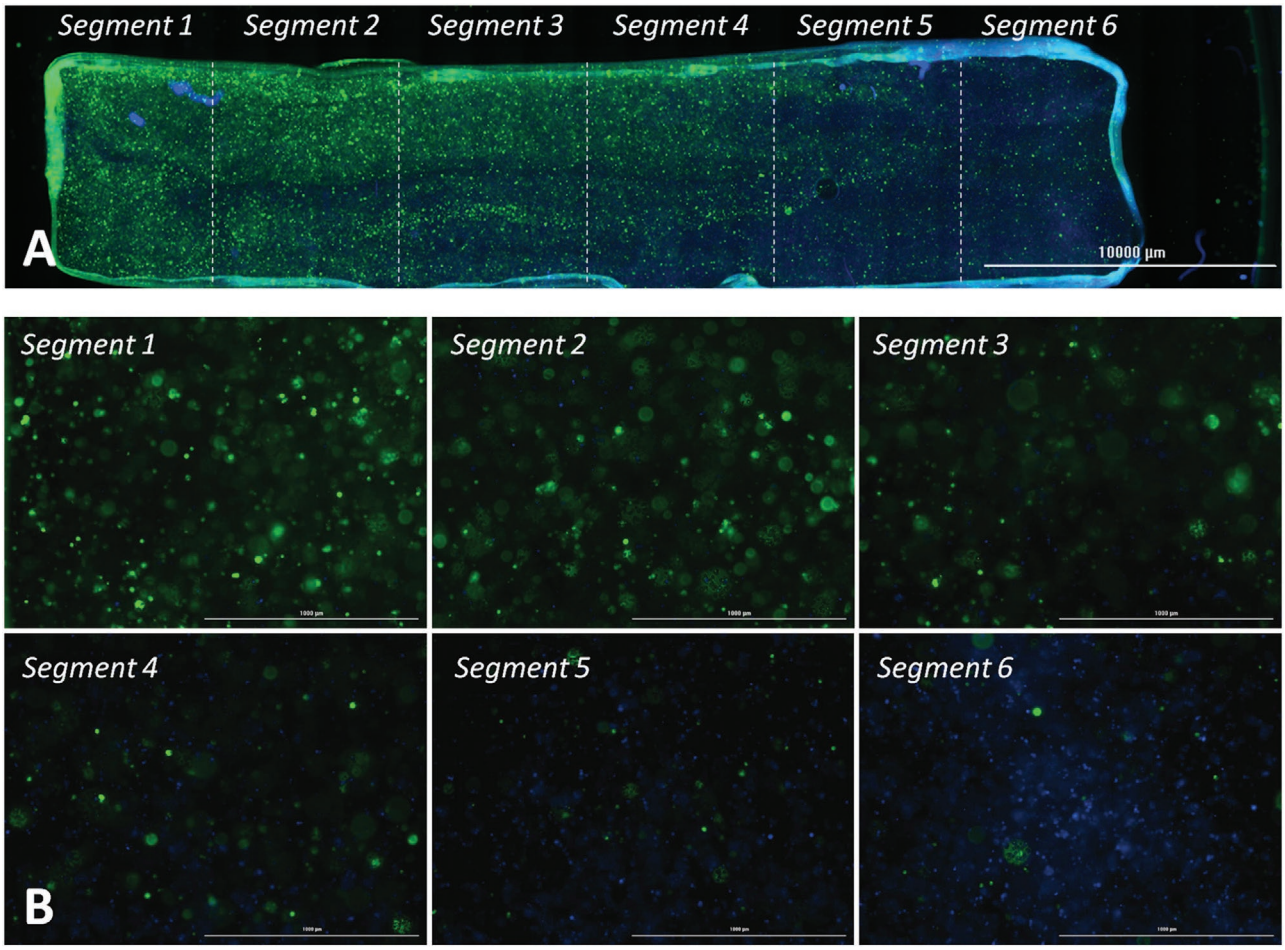

Figure 6. Z-stack projection of the cell-laden stiffness gradient GelMA hydrogel construct after polymerization. A) Overview of the entire gradient construct: HUVECs stained with the blue cell tracker were resuspended in low DoF GelMA and hAD-MSCs stained with green tracker were resuspended in high DoF GelMA. B) Closer view on the cell distribution along the gradient: in the first segment mostly green-stained hAD-MSCs can be observed, and in the last segment mostly the blue stained HUVECs are present.

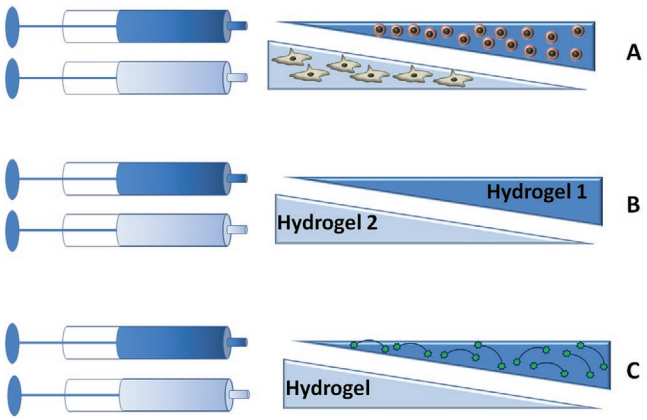

Figure 7. Fabrication of multiple gradients possible by the mixing system: A) gradient of transition from one cell type to another in a co-culture application; B) biochemical gradient by a combination of two hydrogels with different immobilized growth factors, and C) mechanical gradient by increase of crosslinker concentration like the one used in this work.

the gradient (Figure 7B) reveals mostly green-stained hADMSCs in the first segment and mostly blue stained HUVECs in the last segment, with gradient change in proportion of cells along the construct.

The fabrication of gradients for in vitro models and tissue engineered constructs provides researchers with a useful platform of higher complexity, which may be used to recreate the in vivo cell microenvironment. In this work, a stiffness gradient was generated from a photoactive hydrogel by dynamic mixing of precursors with different crosslinker density. The fabrication setup includes a micromixer and a three-pump system, resulting in a versatile system, which can be used to create additional gradient types, by means of mixing specific components in a defined and reproducible manner (Figure 7).

GelMA hydrogels are known to be an excellent tunable tool for hydrogel-based 3D cell culture.[6,33,34] The modified gelatin hydrogels contain inherent bioactive sequences which facilitate ECM-cellular interactions. The mechanical stiffness of GelMA can be manipulated by varying the hydrogel concentration, the photo-crosslinking conditions, and the DoF of the material. It has been demonstrated that GelMA with high DoF has higher stiffness, smaller pore size and lower swelling behavior; by contrast, low DoF GelMA displays very low stiffness, larger pores and high swelling ratio.[35] In general, GelMA materials can be roughly classified according to their DoFs as high, medium or low DoF materials, although there is no scientific consensus as to which DoF range makes up each class.[34,36,37]

There are many different methods to create a stiffness gradient from a photo-crosslinkable hydrogel like GelMA. In general, the procedure follows two steps: 1) the creation of a concentration gradient by varying crosslinker or mass fraction 2) light polymerization (to fix the gradient created in step 1 or to create the gradient itself during step 2 by static or dynamic photopatterning. Various techniques have been described in the literature for the accomplishment of step 1, the creation of a concentration gradient, which then translates into a stiffness gradient. These include i) passive diffusion, ii) convection, iii) microfluidic tree mixers, and iv) dynamic mixing using syringe pumps.[10]

For GelMA, we applied the dynamic mixing strategy with programmable syringe pumps explored earlier by Jeon et al. and Singh et al.[24,29] We chose a mixing method over photo masking for several reasons: 1) we did not want cells to be exposed to variable UV dosage (and free radical concentrations) along the gradient; 2) avoidance of reproducibility issues related to inhomogeneous diffusion of radicals and light penetration depth;[38] and 3) considerations of what constitutes "commonly available" laboratory equipment (syringe pumps, 3D printer, UV crosslinker). An additional advantage conferred by the micromixer system is that it allows for versatile gradient fabrication, as shown in Figure 7. This design flexibility enables the incorporation of other biological and chemical moieties, such as growth factors and additives.

Our strategy represents a combination of dynamic mixing and microfluidics. The syringe pumps are used to create a specific concentration gradient and then a microfluidic micromixer ensures complete mixing with laminar flow. Many groups employ dynamic mixing without providing details of mixing procedure,[23,29,39] or without characterizing if the resulting mixing was truly homogenous.[40,41] However, this is important information, since hydrogels constitute viscous materials and it is important to ensure complete and homogenous mixing of the two precursor solutions. It is also possible to use a commercially available mixer like a spiral mixer,[24] but we wanted to implement a well-characterized mixing device with documented mixing performance, which increases reproducibility between experiments. In this work, we use a sophisticated design that achieves homogeneous mixing of fluids in less than 1 s. In a previous study,[25] we extensively investigated the performance of the micromixer and compared it to various alternative mixer designs. The chosen channel geometry allows homogeneous mixing of fluids by the so-called "split-and-recombine" mechanism. The 3D printed micromixer uses H-shaped channel modules to influence the flow speed at different positions inside the channel, which further enhances mixing. Since commercially available mixers are not well characterized and none of them have been specially adapted for small-scale hydrogel mixing, we believe using 3D printed micromixers will improve the manufacture of reproducible hydrogel gradients. In order to make the designed micromixer system widely available to other working groups, we have also provided a .stl file of the microfluidic device.

The hydrogel gradients created by the micromixer in this work were directly characterized by encapsulation of different fluorescent microbeads in high and low DoF GelMA. We could demonstrate that the amount of green beads decreases in a linear fashion along the gradient fractions, while the fluorescence of the red beads increases. This indicates that the slightly different viscosities of unpolymerized high and low DoF GelMA do not influence the programmed flow profiles. The encapsulated cell gradient marked with cell trackers also showed a rather linear transition between the two cell types. Interestingly, the results of the rheological examination revealed a nonlinear increase of hydrogel stiffness along the fractions. The storage modulus change of the gradient hydrogel, created by the linear mixing profile, can be described as following an exponential trend. The results show that while the mass fraction contribution of each hydrogel remains linear, the presence of additional

methacrylate and methacrylamide groups in the high DoF material leads to an exponential increase in mechanical stiffness. In general, an exponential gradient from 23.7 to 1536.7 Pa could be created in this work. This range can be easily shifted to higher starting values, for example, by using a GelMA with middle range DoF as a starting material in pump 1. Other groups have obtained linear GelMA stiffness gradients by using the photomasking method.[42,43] Pedron et al. have used a microfluidic device for GelMA gradient creation, but they have characterized the gradient along the construct as DoF and not as stiffness directly.[44] In the future, mathematical modeling can be used to better understand this hydrogel behavior and manipulate the pump flow profiles in a manner suitable for the generation of a linear GelMA gradient. Nonlinearity of stiffness, however, should not be a problem, so long as the local elastic moduli are known in each point of the hydrogel. Moreover, most in vivo gradients also do not have a linear profile.[17,44]

A co-culture of hAD-MSCs and HUVECs was encapsulated in the hydrogel gradient fractions, as a proof-of-principle experiment demonstrating the behavior of biological systems in the gradient fractions. The results showed decreased cell spreading with increasing stiffness of the mechanical gradient. Previously, we have shown that high crosslinker density in high DoF GelMA leads to a cell restrictive microenvironment, while hydrogels made of low DoF GelMA contribute to a cell-promoting microenvironment.[6] The exact magnitude of GelMA stiffness, where MSCs cease to spread, however, was previously unknown. The first fractions of gradient GelMA demonstrated extensive MSCs and HUVECs spreading, indicating that cells were able to displace or degrade hydrogel polymer chains. With this experimental setup, we could demonstrate that for hAD-MSCs the range of spreading was situated between 23.7 and 423 Pa. For HUVECs, in contrast, the threshold for spreading was between 23.7 and 125.6 Pa.

Estimation of cell migration in hydrogels plays an important role in the design of tissue engineered constructs. In the case of implantation, vascular ingrowth from the recipient to the graft is an essential part of the entire regeneration progress.[45] Moreover, the possibility of cell migration in the construct might also be a critical factor in terms of establishing intercellular communication and tissue homeostasis[46,47] Evaluation of cell migration in the gradient fractions revealed decreased migration distances with increasing gradient fraction number (and higher stiffness). Similar results were demonstrated for immortalized TERT-hMSCs in fibrin hydrogels of various stiffness, where increased stiffness and decreased pore size limited cell migration.[48]

Cell adhesion, spreading and migration in hydrogels all play a key role in intercellular interactions, as well as neovascularization and material modulation.[49,50] The ability to accurately predict cell behavior in tissue-engineered constructs plays a key role in the success of tissue recreation. Fabrication of gradients can help to find the optimal hydrogel stiffness and composition in order to allow cells to spread and migrate or, alternatively, the technique may be used to entrap cells in a particular construct segment. Indeed, not all cell types require extensive spreading.[51] The developed syringe pump system plus micromixer allows a simple and elegant procedure, which can be used to create a multitude of gradients for studying cell behavior in photo-crosslinkable hydrogels like GelMA, and can be used for exploring variable composition of cellular niches.

4. Conclusions

This study reports the fabrication and characterization of GelMA gradient hydrogels, created by dynamic mixing of low DoF and high DoF hydrogels. We demonstrate that the unpolymerized hydrogels were mixed according to the programmed flow profiles. Although a linear increase or decrease of the flows of the different hydrogels was performed, the resulting gradient had an exponential function in terms of stiffness. Through the creation of a transitional stiffness gradient range between low and high DoF GelMA, differences in cell behavior of hAD-MSCs and HUVECs could be observed. Taken together, our work demonstrates an elegant technique for the fabrication of GelMA hydrogel stiffness gradients and provides an example of a versatile 3D printed micromixer. With the help of the described system, GelMA gradient constructs can be created and optimal 3D cell culture conditions can be experientially identified for mono- or co-cultured cells.

Supporting Information

Supporting Information is available from the Wiley Online Library or from the author.

Acknowledgements

This research was supported by the German Research Foundation (DFG Project 398007461 488 3D Dual-Gradient Systems for Functional Cell Screening) and partly funded via the DFG Emmy Noether programme, project ID 346772917. The support by the SMART BIOTECS initiative, financially supported by the Ministry of Science and Culture (MWK) of Lower Saxony, Germany is also acknowledged. The publication of this article was funded by the Open Access Fund of Leibniz Universität Hannover. The confocal laser scanning microscope was funded by the Deutsche Forschungsgemeinschaft (DFG, German Research Foundation) – 420505864.

Conflict of Interest

The authors declare no conflict of interest.

Keywords

3D cell cultures, 3D printing, gelatin-methacryloyl hydrogel, microfluidic mixers, stiffness gradients

Received: April 2, 2020
Revised: May 20, 2020
Published online: June 15, 2020

[1] S. Diederichs, S. Bohm, A. Peterbauer, C. Kasper, T. Scheper, M. van Griensven, *J. Biomed. Mater. Res., Part A* **2010**, *94*, 927.

[2] F. Guilak, D. M. Cohen, B. T. Estes, J. M. Gimble, W. Liedtke, C. S. Chen, *Cell Stem Cell* **2009**, *5*, 17.
[3] R. M. Delaine-Smith, G. C. Reilly, *Muscles Ligaments Tendons J.* **2012**, *2*, 169.
[4] R. A. Marklein, J. A. Burdick, *Soft Matter* **2010**, *6*, 136.
[5] R. A. Marklein, D. E. Soranno, J. A. Burdick, *Soft Matter* **2012**, *8*, 8113.
[6] I. Pepelanova, K. Kruppa, T. Scheper, A. Lavrentieva, *Bioengineering* **2018**, *5*, 55.
[7] F. Ruedinger, A. Lavrentieva, C. Blume, I. Pepelanova, T. Scheper, *Appl. Microbiol. Biotechnol.* **2015**, *99*, 623.
[8] M. M. Benmassaoud, K. A. Gultian, M. DiCerbo, S. L. Vega, *Ann. N. Y. Acad. Sci.* **2020**, *1460*, 25.
[9] J. Yang, Y. S. Zhang, K. Yue, A. Khademhosseini, *Acta Biomater.* **2017**, *57*, 1.
[10] S. Sant, M. J. Hancock, J. P. Donnelly, D. Iyer, A. Khademhosseini, *Can. J. Chem. Eng.* **2010**, *88*, 899.
[11] J. Wu, Z. Mao, H. Tan, L. Han, T. Ren, C. Gao, *Interface Focus* **2012**, *2*, 337.
[12] L. Wang, Y. Li, G. Huang, X. Zhang, B. Pingguan-Murphy, B. Gao, T. J. Lu, F. Xu, *Crit. Rev. Biotechnol.* **2016**, *36*, 553.
[13] T. Xia, W. Liu, L. Yang, *J. Biomed. Mater. Res., Part A* **2017**, *105*, 1799.
[14] M. S. Laasanen, J. Toyras, R. K. Korhonen, J. Rieppo, S. Saarakkala, M. T. Nieminen, J. Hirvonen, J. S. Jurvelin, *Biorheology* **2003**, *40*, 133.
[15] E. S. Place, N. D. Evans, M. M. Stevens, *Nat. Mater.* **2009**, *8*, 457.
[16] G. M. Fomovsky, J. W. Holmes, *Am. J. Physiol.: Heart Circ. Physiol.* **2010**, *298*, H221.
[17] E. Moeendarbary, I. P. Weber, G. K. Sheridan, D. E. Koser, S. Soleman, B. Haenzi, E. J. Bradbury, J. Fawcett, K. Franze, *Nat. Commun.* **2017**, *8*, 14787.
[18] Z. Chen, X. Luo, X. Zhao, M. Yang, C. Wen, *J. Orthop. Transl.* **2019**, *17*, 55.
[19] H. Jo, M. Yoon, M. Gajendiran, K. Kim, *Macromol. Biosci.* **2020**, *20*, 1900300.
[20] T. Xia, W. Liu, L. Yang, *J. Biomed. Mater. Res., Part A* **2017**, *105*, 1799.
[21] L. G. Vincent, Y. S. Choi, B. Alonso-Latorre, J. C. Del Álamo, A. J. Engler, *Biotechnol. J.* **2013**, *8*, 472.
[22] D. Lee, K. Golden, M. M. Rahman, A. Moran, B. Gonzalez, S. Ryu, *Exp. Mech.* **2019**, *59*, 1249.
[23] M. C. Mosley, H. J. Lim, J. Chen, Y. H. Yang, S. Li, Y. Liu, L. A. Smith Callahan, *J. Biomed. Mater. Res., Part A* **2017**, *105*, 824.
[24] O. Jeon, D. S. Alt, S. W. Linderman, E. Alsberg, *Adv. Mater.* **2013**, *25*, 6366.
[25] A. Enders, I. G. Siller, K. Urmann, M. R. Hoffmann, J. Bahnemann, *Small* **2019**, *15*, 1804326.
[26] V. Viktorov, M. R. Mahmud, C. Visconte, *Chem. Eng. Res. Des.* **2016**, *108*, 152.
[27] I. G. Siller, A. Enders, T. Steinwedel, N.-M. Epping, M. Kirsch, A. Lavrentieva, T. Scheper, J. Bahnemann, *Materials* **2019**, *12*, 2125.
[28] H. Shirahama, B. H. Lee, L. P. Tan, N.-J. Cho, *Sci. Rep.* **2016**, *6*, 31036.
[29] M. Singh, C. P. Morris, R. J. Ellis, M. S. Detamore, C. Berkland, *Tissue Eng., Part C* **2008**, *14*, 299.
[30] J. Huff, A. Bergter, B. Luebbers, *Multiplex Mode for the LSM 9 Series with Airyscan 2: Fast and Gentle Confocal Super-Resolution in Large Volumes*, Nature Publishing Group, England **2019**.
[31] A. A. Khalil, P. Friedl, *Integr. Biol.* **2010**, *2*, 568.
[32] J. A. Burdick, A. Khademhosseini, R. Langer, *Langmuir* **2004**, *20*, 5153.
[33] Y. C. Chen, R. Z. Lin, H. Qi, Y. Yang, H. Bae, J. M. Melero-Martin, A. Khademhosseini, *Adv. Funct. Mater.* **2012**, *22*, 2027.
[34] D. Loessner, C. Meinert, E. Kaemmerer, L. C. Martine, K. Yue, P. A. Levett, T. J. Klein, F. P. Melchels, A. Khademhosseini, D. W. Hutmacher, *Nat. Protoc.* **2016**, *11*, 727.
[35] M. Kirsch, L. Birnstein, I. Pepelanova, W. Handke, J. Rach, A. Seltsam, T. Scheper, A. Lavrentieva, *Bioengineering* **2019**, *6*, 76.
[36] J. W. Nichol, S. T. Koshy, H. Bae, C. M. Hwang, S. Yamanlar, A. Khademhosseini, *Biomaterials* **2010**, *31*, 5536.
[37] A. I. Van Den Bulcke, B. Bogdanov, N. De Rooze, E. H. Schacht, M. Cornelissen, H. Berghmans, *Biomacromolecules* **2000**, *1*, 31.
[38] W. J. Hadden, J. L. Young, A. W. Holle, M. L. McFetridge, D. Y. Kim, P. Wijesinghe, H. Taylor-Weiner, J. H. Wen, A. R. Lee, K. Bieback, *Proc. Natl. Acad. Sci. USA* **2017**, *114*, 5647.
[39] L. A. S. Callahan, A. M. Ganios, E. P. Childers, S. D. Weiner, M. L. Becker, *Acta Biomater.* **2013**, *9*, 6095.
[40] S. Nemir, H. N. Hayenga, J. L. West, *Biotechnol. Bioeng.* **2010**, *105*, 636.
[41] S. A. DeLong, J. J. Moon, J. L. West, *Biomaterials* **2005**, *26*, 3227.
[42] C. Kim, J. L. Young, A. W. Holle, K. Jeong, L. G. Major, J. H. Jeong, Z. M. Aman, D.-W. Han, Y. Hwang, J. P. Spatz, *Ann. Biomed. Eng.* **2020**, *48*, 893.
[43] C. D. O'Connell, B. Zhang, C. Onofrillo, S. Duchi, R. Blanchard, A. Quigley, J. Bourke, S. Gambhir, R. Kapsa, C. Di Bella, *Soft Matter* **2018**, *14*, 2142.
[44] S. Pedron, E. Becka, B. A. Harley, *Adv. Mater.* **2015**, *27*, 1567.
[45] J. C.-Y. Chung, D. Shum-Tim, *Cells* **2012**, *1*, 1246.
[46] B. Mattes, S. Scholpp, *Histochem. Cell Biol.* **2018**, *150*, 431.
[47] M. Miller, M. Hafner, E. Sontag, N. Davidsohn, S. Subramanian, P. E. Purnick, D. Lauffenburger, R. Weiss, *PLoS Comput. Biol.* **2012**, *8*, e1002579.
[48] N. Salam, S. Toumpaniari, P. Gentile, A. Marina Ferreira, K. Dalgarno, S. Partridge, *Materials* **2018**, *11*, 1781.
[49] S. R. Caliari, S. L. Vega, M. Kwon, E. M. Soulas, J. A. Burdick, *Biomaterials* **2016**, *103*, 314.
[50] U. Blache, M. Ehrbar, *Adv. Wound Care* **2018**, *7*, 232.
[51] E. M. Ovadia, D. W. Colby, A. M. Kloxin, *Biomater. Sci.* **2018**, *6*, 1358.